J Electroceram (2009) 23:150–153
DOI 10.1007/s10832-007-9343-8

Enhanced of electrical characteristics of nano-crystal floating gate memory with In_2O_3 nano-particles embedded in polyimide

Hyun-Mo Koo · Won-Ju Cho · Dong Uk Lee · Seon Pil Kim · Eun Kyu Kim

Received: 31 May 2007 / Accepted: 8 October 2007 / Published online: 23 October 2007

Abstract We fabricated the nano-floating gate memory (NFGM) with In_2O_3 nano-particles embedded in polyimide gate insulators. Self-assembled In_2O_3 nano-particles were created by chemical reaction between the polymer precursor and the indium film. The particle size and density of In_2O_3 nano-particles were about 7 nm and 6×10^{11} cm^{-2}, respectively. The electrical characterization of the NFGM with In_2O_3 nano-particles embedded in polyimide layer were measured and the memory window larger than 3.8 V was obtained from the fabricated NFGM devices due to the charging effects of In_2O_3 particles. Subthreshold swing, output current characteristics and retention time of fabricated NFGM devices were considerably improved by the post-annealing process in 3% hydrogen diluted H_2/N_2 ambient.

Keywords Nano-floating gate memory · In_2O_3 metal nano-particles · Annealing effect · Post-annealing

1 Introduction

The flash memory devices have an important position in semiconductor industry because it has the capability of non-volatile storage with a large memory capacity and a fast access time comparable to dynamic random access memories [1]. Nano-sized quantum structure has been attractive candidate for investigations of fundamental physical property and for potential applications in the next-generation electronic devices. Also, a non-volatile memory device holds a key post in the semiconductor industry, because of increasing demands for information storage [2]. Especially, the metal nano-particles have some advantages such as higher density of states around the Fermi level with a smaller energy perturbation. Furthermore, the metal nano-particles form the deep quantum wells between control oxide and tunnel oxide due to the difference of work functions [3, 4]. In recent years, a new nano-floating gate memory device has been studied using metal oxide nano-particles and polyimide layers as charge storage layer and gate insulator, respectively [5]. The polyimide has a potential matrix for the nano-particles because of its good thermal stability and chemical endurance for electric and optoelectronic applications [6]. It is reported that the Cu_2O, ZnO, Fe_2O_3 or $Ni_{1-x}Fe_x$ metal nano-particles embedded in polyimide layer were produced during the imidization of polyimide precursors [7–10]. Particularly, the In_2O_3 nano-particles in polyimide layer have received much attention due to the nano-device applications like floating gated memories and quantum-dot tunneling devices.

In this study, We have formed In_2O_3 nano-particles embedded in a polyimide layer by using selective reaction of indium film, and electrical properties of NFGM based on the In_2O_3 nano-particles were performed to investigate the memory effect of the nano-composites. Additionally, a post-annealing process in 3% hydrogen diluted H_2/N_2 ambient was carried out in order to improve the performance of NFGM devices.

H.-M. Koo (✉) · W.-J. Cho
Department of Electronic Materials Engineering,
Kwangwoon University,
Seoul 139-701, South Korea
e-mail: chowj@kw.ac.kr

D. U. Lee · S. P. Kim · E. K. Kim
Department of Physics, Hanyang University,
Seoul 133-791, South Korea

2 Experimental

The floating gate memory with In_2O_3 nano-particles in polyimide gate insulator layer were fabricated on the p-type (100) UNIBOND silicon-on-insulator (SOI) wafers with a 100 nm top Si layer and a 200 nm buried oxide layer. Silicon active region was produced by photolithography and plasma reactive ion etching (RIE) processes. After formation of tunneling gate oxide with a thickness of 4.5 nm by dry oxidation, the deposition of indium layer with 5-nm-thick by thermal evaporator and the spin coating of polyamic acid (PAA) with a 50 nm thickness were sequentially followed. The PAA used in this work is a commercial biphenyltertracarboxylic dianhydride-phenylen diamin (BPDA-PDA) type (Dupont PI2610D) and is composed of BPDA-PDA in *N*-methyl-2-pyrrolidone (3 wt%). The PAA and the indium were maintained at room temperature for 24 h for the formation of indium ions by chemical reactions between indium ion and PAA. The curing process was carried out at 400 °C for 1 h after baking of 135 °C for 30 min in a rapid thermal process (RTA) system in N_2 atmosphere. The In_2O_3 nano-particles were formed inside polyimide matrix during the curing process by chemical reaction of indium ions and PAA. The aluminum was deposited by thermal evaporation and gate electrode was formed by photolithography and aluminum etching. Finally, the fabricated devices were annealed in 3% diluted hydrogen (H_2/N_2) ambient at 400 °C for 30 min to improve the electrical characteristics.

3 Results and discussion

Figure 1 shows the cross-section schematic of fabricated NFGM devices with In_2O_3 nano-particles embedded in polyimide layer. The channel length and width of NFGM are 10 and 20 μm, respectively. The gate stacks consisted of 4.5-nm-thick SiO_2 tunnel oxide/7-nm-diameter In_2O_3 nano-particles/50-nm-thick polyimide control insulator/150-nm-thick Al electrode.

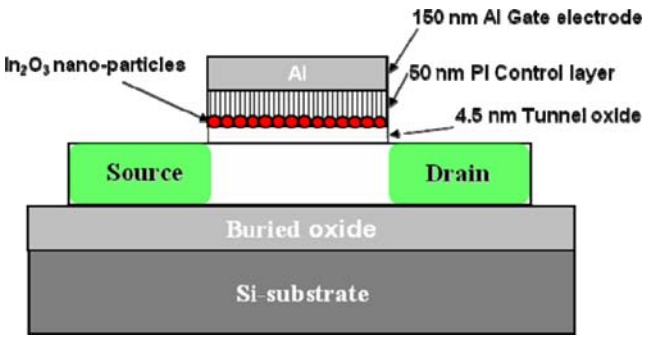

Fig. 1 Cross-sectional schematic of fabricated NFGM with In_2O_3 nano-particles embedded in polyimide layer

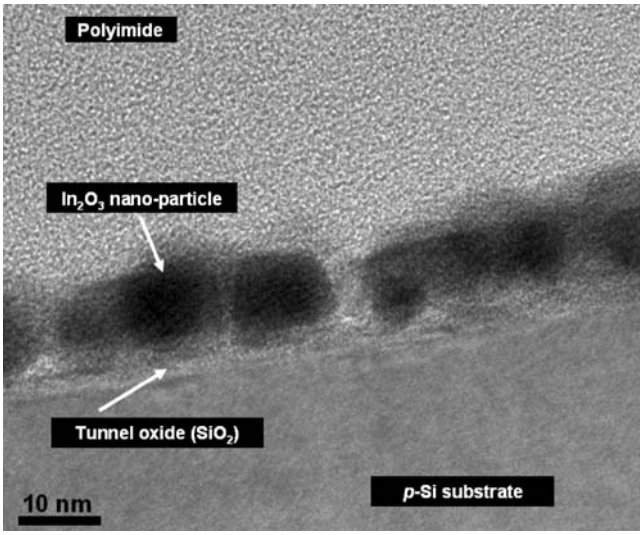

Fig. 2 Cross-sectional TEM image of In_2O_3 nano-particles embedded in polyimide layer

Figure 2 shows the cross-sectional TEM image of In_2O_3 nano-particles embedded in polyimide layer after curing process of 400 °C for 1 h. It is found that the nano-particles have a spherical shape with an average diameter of 7 nm and a particle density of 6×10^{11} cm^{-2}. Also, the thicknesses of tunnel oxide and polyimide insulator were about 4.5 and 50 nm, respectively. The uniformity of In_2O_3 nano-particles was analyzed by plane-view TEM and a relatively uniform distribution across the films was confirmed.

Figure 3 shows the molecular structure of BPDA-PDA after the curing process at 400 °C for 1 h. The In_2O_3 nano-particles were created from the chemical reaction of

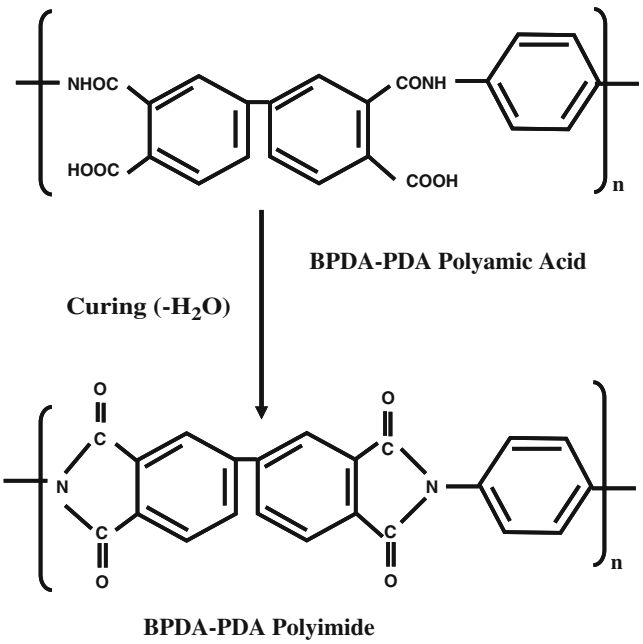

Fig. 3 Molecular structure of BDPA-PDA type polyimide after curing process

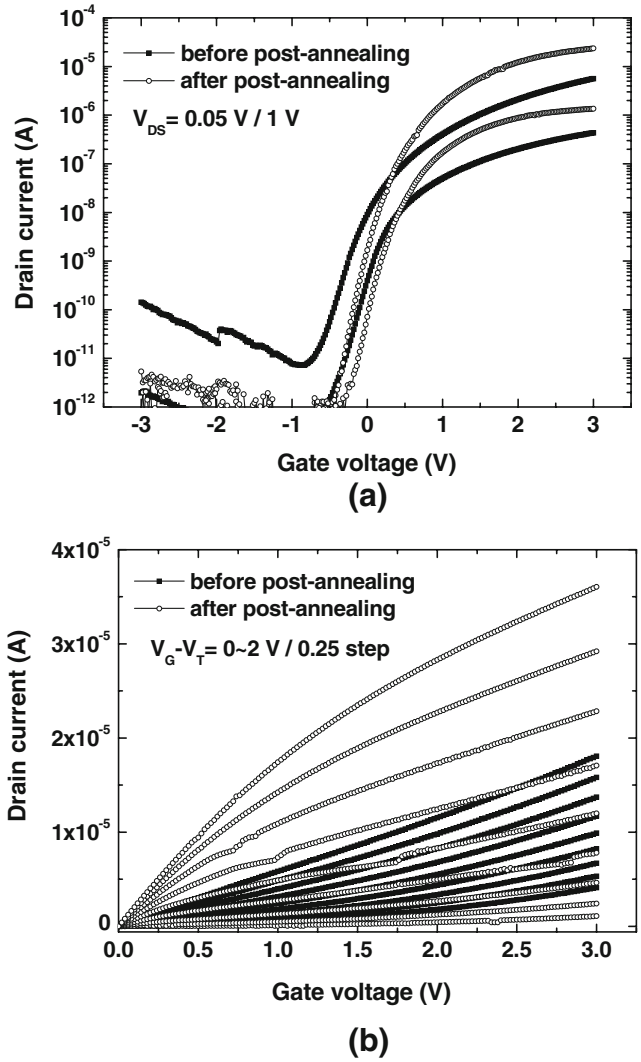

Fig. 4 Subthreshold characteristics (**a**) and output current characteristics (**b**) of fabricated NFGM with In_2O_3 nano-particles embedded in polyimide layer

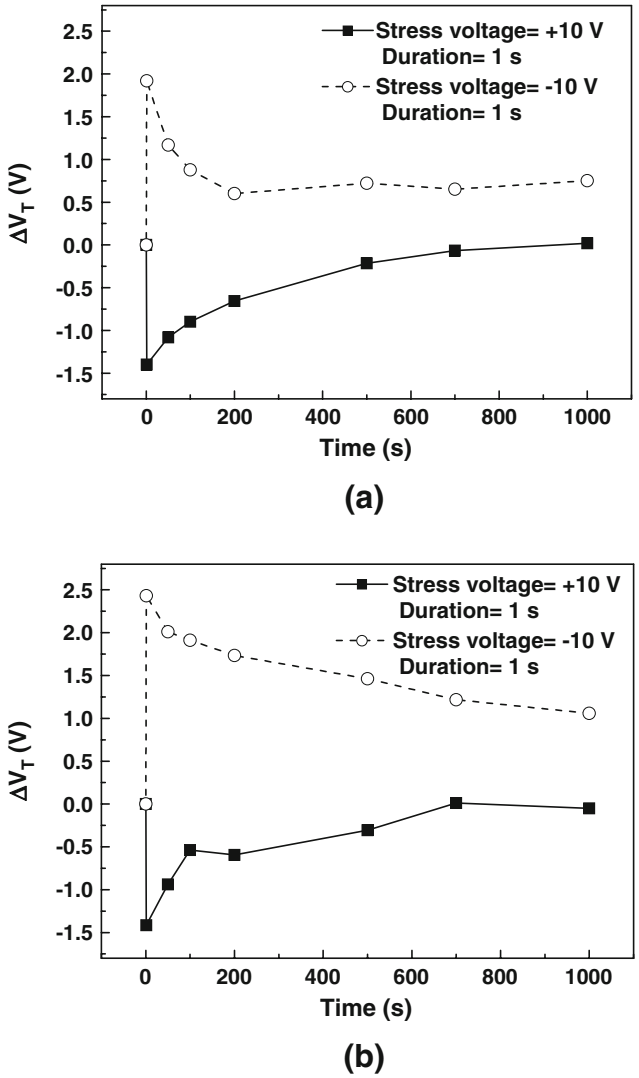

Fig. 6 Retention time characteristics of fabricated NFGM with In_2O_3 nano-particles embedded in polyimide layer (**a**) and after post-annealing of 3% hydrogen diluted (H_2/N_2) gas (**b**)

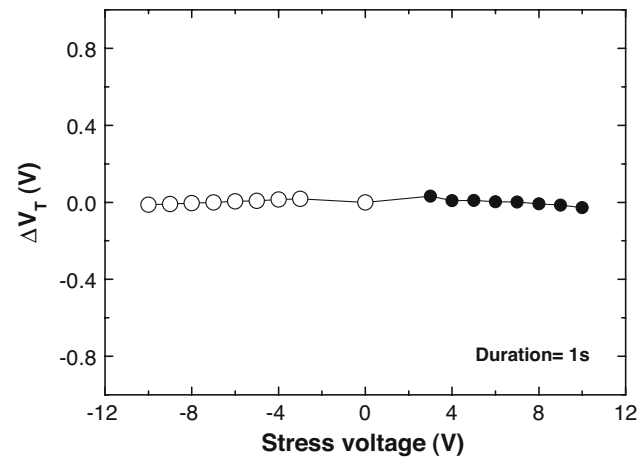

Fig. 5 Threshold voltage shift characteristics for voltage of NFGM without In_2O_3 nano-particles

deposited indium and polyamic acid in polyimide matrix during the curing process of BPDA-PDA and the dielectric constant of BPDA-PDA Polyimide is known as 2.9~3.2 [11, 12].

Figure 4 shows the subthreshold characteristics and the output current characteristics of the fabricated NFGM with In_2O_3 nano-particles in polyimide. It is found that the electrical characteristics are considerably improved after annealing of 3% diluted hydrogen (H_2/N_2) ambient at 400 °C for 30 min. The threshold voltage was changed from 1 to 0.2 V and the subthreshold swing decreased from 200 to 120 mV/dec. Also, the leakage currents at the negative gate biased region were considerably reduced as shown in Fig. 4(a) and the output current at positive gate biases increased as shown in Fig. 4(b).

In order to evaluate the origin of charging effect in In_2O_3 nano-particles, the NFGM devices without In_2O_3 nano-

particles were also fabricated and the charging effect was compared. Figure 5 shows the threshold voltage shift characteristics for the stress voltage of NFGM devices without In_2O_3 nano-particles. Even though the stress voltage changed from −10 to 10 V, the shift of threshold voltage was not observed. Therefore, it is concluded that the charging effect is not originated from the tunnel oxide/polyimide insulator layers but comes from the In_2O_3 nano-particles.

Figure 6 shows charge retention characteristics of the fabricated NFGM with In_2O_3 nano-particles embedded in polyimide layer and the dependence of charge retention characteristics on the post-annealing. Before the post-annealing, the memory window of initial state was about 3.3 V as shown in Fig. 6(a). But the memory window rapidly decreased with the increasing time. After 10^3 s, the memory window was reduced to 0.6 V. On the other hand, the charge retention characteristics were considerably improved after 3% hydrogen diluted (H_2/N_2) ambient post-annealing processes as show in Fig. 6(b). The memory window of initial state was about 3.8 V and maintained 1.1 V after 10^3 s. It is considered that such improvements would be associated with the reduction of interface traps at the tunnel oxide/polyimide interface and bulk traps in polyimide layer [13].

4 Conclusion

The NFGM devices with In_2O_3 nano-particles embedded in BPDA-PDA polyimide layer were fabricated. The In_2O_3 nano-particles have spherical shape with an average diameter of 7 nm and the particle density was 6×10^{11} cm^{-2}. The tunnel oxide and control polyimide insulator layer were 4.5 and 50 nm. The post-annealing in 3% diluted hydrogen (H_2/N_2) ambient at 400 °C for 30 min significantly improved the electrical characteristics of In_2O_3 nano-particles embedded NFGM. Therefore, the NFGM devices with In_2O_3 nano-particles embedded in polyimide are believed to be next generation non-volatile memory devices with high performance and integration density.

Acknowledgements The present Research has been conducted by the Research Grant of Kwangwoon University in 2007.

References

1. W.D. Brown, J.E. Brewer, *Nonvolatile Semiconductor Memory Technology: A Comprehensive Guide to Understanding and Using NVSM Devices* (IEEE Press 1998), p. 189
2. A.K. Sharma, *Advanced semiconductor memories : Architectures, Designs, and Applications* (IEEE Press, John Wiley & Sons, 2003), p. 596
3. Z. Liu, C. Lee, V. Narayanan, G. Pei, E.C. Kan, IEEE Trans. Electron Dev. **49**, 1606 (2002)
4. Dong Uk Lee, Min Seung Lee, Jae.-Hoon Kim, Eun kyu Kim, Appl. Phys. Lett. **90**, 093514 (2007)
5. D.H. Zhang, C. Li, S. Han, X.L. Liu, T. Tang, W. Jin, C.W. Zhou, Appl. Phys. Lett. **82**, 112 (2003)
6. Y. Chung, H.P. Park, H.J. Jeon, C.S. Yoon, S.K. Kim, Y.-H. Kim, J. Vac. Sci. Technol. B. **21**, L9 (2003)
7. Y.-H. Kim, G.F. Walker, J. Kim, J. Park, J. Adhes. Sci. Technol. **1**, 331 (1987)
8. J.H. Jung, J.H. Kim, T.W. Kim, C.S. Yoon, Y.-H. Kim, S. Jin, Appl. Phys. Lett. **89**, 022112 (2006)
9. J.H. Kim, J.Y. Jin, J.H. Jung, I. Lee, T.W. Kim, S.K. Kim, C.S. Yoon, Y.-H. Kim, Appl. Phys. Lett. **86**, 032904 (2005)
10. E.K. Kim, J.-H. Kim, D.U. Lee, G.H. Kim, Y.-H. Kim, Jpn. J. Appl. Phys. **45**, 7209 (2006)
11. D.U. Lee, J.-H. Kim, E.K. Kim, J. Korean Phys. Soc. **49**, 1188 (2006)
12. M.H. Yi, W. Huang, M.Y. Jin, K.Y. Choi, Macromolecules. **30**, 5606 (1997)
13. W.-J. Cho, C.-G. Ahn, Appl. Phys. Lett. **90**, 143509 (2007)